processes

MDPI

Article

Bioenvironmental Zonal Controlling of Incubated Avian Embryo Using Localised Infrared Heating

Ali Youssef, Tomas Norton * and Daniel Berckmans

Department of Biosystems, Animal and Human Health Engineering Division, M3-BIORES: Measure, Model & Manage of Bioresponses Laboratory, KU Leuven, Kasteelpark Arenberg 30, 3001 Heverlee, Belgium; ali.youssef@kuleuven.be (A.Y.); daniel.berckmans@kuleuven.be (D.B.)

* Correspondence: tomas.norton@kuleuven.be

Received: 25 August 2019; Accepted: 17 September 2019; Published: 23 September 2019

Abstract: The main objective of any bioenvironmental controller is to create favourable bioenvironmental conditions around the living-system. In industrial incubation practice of chicken embryo, it is sometimes difficult to fill large incubators with uniform eggs, which leads to suboptimal results. The ideal incubation solution is a machine that is capable of coping with all sorts of variabilities in eggs. This can be realised in practice by creating different zones of different environmental conditions within the same machine. In the present study, a two-levels controller was designed and implemented to combine both convective and radiative heating to incubate eggs. On the higher level, three model-predictive-control (MPC) constrained controllers were developed to regulate the power applied to nine IR-radiators divided into three zones based on continuous feedback of the eggshell temperatures in each zone. On the lower level, a PID controller was used to maintain the air temperature within an experimental incubator at a fixed level (34 °C) lower than the standard incubation temperature. Four full incubation trials were carried out to test and implement the developed zonal controllers. The implementation results showed that the developed controllers were able to follow the reference trajectory defined for each zone. It was possible to keep the eggshell temperatures within the middle region (zone) different from the sidelong regions (zones) while the air temperature kept constant at 34 °C. The average hatching result (HOF) of the four full incubation trial was 84.0% (±0.5). The developed two-levels control system is a promising technique for demand-based climate controller and to optimizing energy use by using multi-objectives MPCs with constraint on total energy consumption.

Keywords: bioenvironmental control; model-predictive controller; zonal controlling; dynamic modelling

1. Introduction

The production of meat and eggs worldwide is increasing because of the growing population and the high demand of animal proteins [1]. In the poultry industry, meat and egg production sectors require large-scale incubation of eggs at a hatchery and a well-controlled and monitored environment [2].

Eggs of different origins and with different pre-incubation treatments are put together in an incubator, resulting in a non-uniformity between the hatching times of the different eggs [3]. This non-synchronised time of hatch, referred to as a large hatch window, is negative in terms of animal welfare and post-hatching performance, as the chicks are deprived from food and water (until the rest of the eggs are hatched and transferred to the farm) [4–7]. Hatcheries therefore have a strong objective to synchronise the hatch time.

In practice, the incubation process takes place in two different machines, namely, (i) the setter (from incubation day 0 to day 16–18) where the embryos stay during the largest part of their development and (ii) the hatcher (day 17–19 to day 20) where the embryos hatch.

In practice, today's tendency is that incubators are becoming larger. This has however implications on hatchery management. In practice, as hen houses are not increasing in size, it becomes more difficult to fill such larger incubators with uniform eggs from a single flock and storage time. Therefore, it regularly happens that eggs from two or three different flocks are combined in one machine, which can lead to sub-optimal results. For instance, putting eggs from a flock with an age of 30 weeks with those from another flock of 60 weeks of age in the same incubator will certainly lead to a decrease in the number of hatched chicks, poorer chick quality, higher post-hatch mortality, etc., under present conditions where all eggs in the machine are treated equally [8–10].

The ideal incubation solution is a machine that is capable of coping with all sorts of variabilities in eggs (e.g., flock age, strain, storage time, etc.,). This can be realised in practice by creating different zones with different environmental conditions within the same machine. Localised manipulation of the environmental variables inside the incubator (mainly temperature) is a potential solution to create different zones within the incubator space. The creation of different temperature zones by means of air-heat flow control is a very complex and expensive process [11–14]. The best option, according to many scientists, is the radiation (radiant) method of heating. In practice, for the creation of localized zones with a higher temperature, heating systems based on electric radiation (infrared) heaters have been widely used [11]. Radiation (infrared) heating systems radiantly heat surfaces rather than air volumes, which allows them to be used to heat individual zones of eggs, which cannot be achieved with conventional forced convective heating.

During incubation, the thermoregulatory system of the chicken embryo evolves through different stages from a poikilothermic to a homeothermic system [15,16]. The incubated egg is considered as a complex, individually different, time varying and dynamic (CITD) system as introduced by Berckmans et al. (e.g., [15,17,18]). Hence, the dynamic thermal response of the fertile egg to changes in ambient temperature is different from one day to another during the embryonic development [15]. As such, modelling and controlling a biological system such as the fertile incubated eggs is more complex than modelling of non-living physical systems (such as electric circuits). Most of the biological responses including heat production of incubated eggs are results of a complex network of interactions among many components inside the egg. We have ([12]) successfully implemented the multi-zonal controlling in an empty ventilated chamber using a multi-objective proportional-integral-plus (PIP). However, implementing such multi-zonal controller in a bio-environment around living systems (e.g., incubated embryo) is a great challenge because of the inherent non-linearity of the system. One of the challenges that are engaged with controlling different thermal zones simultaneously (multi-zonal control) is the controllability of the system under question. The controllability property of the system plays a crucial role in many control problems, such as stabilization of unstable systems by feedback, or optimal control [19,20]. The system's controllability can be roughly defined as an ability to do whatever we want with our system, or in more technical terms, the ability to transfer our system from any initial state to any desired final state in a finite time [18]. The challenge facing us to control multi-thermal-zones was to control the temperature in a certain number of zones inside the test chamber with a minimal number of control variables. Model-based control techniques, such as model-predictive-control (MPC) are suitable approaches to handle the inherent nonlinearity of the living systems and the interaction of the different thermal zones. The MPC is well-known and frequently used in the industry for optimal control of time-varying systems with constraints [21]. MPC benefits from simple and intuitive tuning and the ability to control a range of simple and complex phenomena, including systems with time delays, non-minimum phase dynamics, and instability [22]. Additionally, the framework of MPC incorporates straightforwardly system's constraints and multiple operating conditions, exhibits an intrinsic compensation for dead time, and provides the flexibility to formulate and tailor a control objective [21,22].

The main objective of this paper is to investigate the possibility of zonal controlling the bio-environment of incubated chicken embryo by combining forced convection and localised infrared heat using adaptive predictive-controlling approach.

2. Materials and Methods

2.1. Experimental Setup

2.1.1. Experimental Incubator

Experiments were carried out in a small-scale experimental incubator (see Figure 1) at the division of Measure, Model and Manage Bio-responses (M3-BIORES), Leuven University (KU Leuven), Belgium. The experimental incubator is composed of the main chamber and the air preparation chamber whose inner dimension is 0.8 × 0.6 × 0.4 m and 0.8 × 0.25 × 0.4 m (l × w × h), respectively (Figure 1). Both chambers have 0.04 m thick surrounding walls made of propylene. The air preparation chamber is equipped with an air re-circulation, one inlet opening for fresh air, four re-circulation openings, and a pipe system (Figure 1) with a three-way valve to regulate the flow rate of fresh air (refreshment) and re-circulated air coming from the main chamber. The fresh air and re-circulated air were mixed within the air preparation chamber to be pumped into the main chamber through two inlet pipes (Figure 1). Volumetric flow rate, of fresh air versus that of the re-circulated air, into the main chamber is conditioned by the open degree of the three-way valve. With 100% valve open, maximum ventilation rate of 0.17 m^3 h^{-1} (0.885 volume refreshment per hour) was achieved with no air re-circulation. The main chamber is equipped with two heater fans connected to the two inlet pipes, which create forced air ventilation and supply maximum total heat of 200 W in the system (Figure 1). The prepared air (in the air preparation chamber) is pumped through the heater fan to be heated up, if the heaters were on, before flowing into the main chamber (Figure 1). The air inside the main chamber is exhausted through the four openings on the top sidewall. Portion of the exhausted air (based on the control suggestion) was mixed with the fresh inlet air and the rest was removed out of the incubator through the main outlet opening. A mixing fan was positioned in the middle of the main chamber to accelerate the mixing of the inlet air with the air inside the chamber. The main chamber was designed to hold a standard incubation egg tray above the mixing fan and the air inlet pipes. The used egg tray was a Petersime N.V. standard setter tray (B00568) for chicken eggs with 150 egg places arranged in a 10 × 15 matrix and made of polypropylene. Air temperature, eggshell temperature and relative humidity inside the test chamber were automatically controlled using the Petersime Focus^{TM} controller. Control actions are calculated based on continuous feedback from a temperature/humidity probe, which is placed inside the main chamber. The controller compares the measurements from these sensors with the set points to make the decision of heating up by turning on the heater fan, cooling down by cool air ventilation or humidifying by supply steam from the steam generator or dehumidifying by dry air ventilation. The Petersime Focus^{TM} control box is connected to the data acquisition and control PC where the incubation process and control actions were programmed using the Petersime Focus Software (v.2.0).

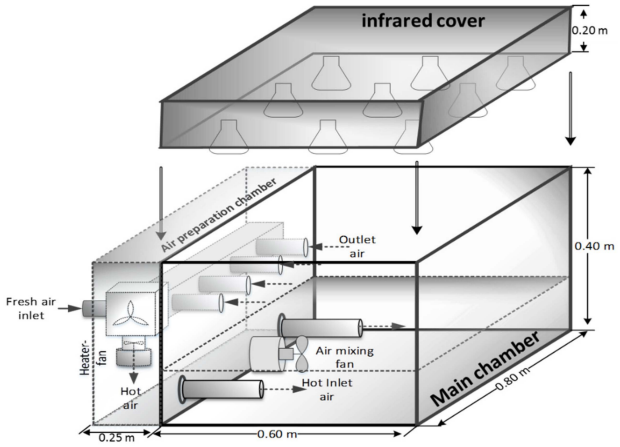

Figure 1. Schematic representation of the experimental incubator showing the main chamber, air preparation chamber, and the infrared cover.

2.1.2. Infrared Cover

The cover of the experimental incubator was designed to provide infrared heating in the top of the incubated eggs. The infrared cover was equipped of nine ceramic infrared (IR) radiators (lamps), of the type Elstein® IOT/75. The used Elstein IOT/75 lamps were ceramic infrared dark radiators with maximum power of 100 Watts and operating infrared wavelength range of 3–10 μm. The IR lamps were equipped with E27 threads that can be screwed-in like bulbs into porcelain sockets. Nine porcelain sockets were fixed on three metal bars with three sockets each (Figure 2). The three metal bars were fixed to the inner side of a wooden frame (with an inner dimension 0.8 × 0.60 × 0.20 m) in such a way that the IR lamps were facing downward (Figure 2). The distance (*h*) between the IR lamps and the eggs was adjustable, within the range h = 0.1 and 0.3 m, using four adjustment knobs (Figure 2, top view). A plexiglass cover was placed on the top of the wooden frame. A rubber washer was placed between the wooden frame and the incubator chamber to prevent air leakage. The nine IR lamps were divided into three groups, each consisting of three IR lamps. The power applied to each of the three groups were individually controlled via a model-predictive-controller (MPC) designed for this purpose (see Section 2.4).

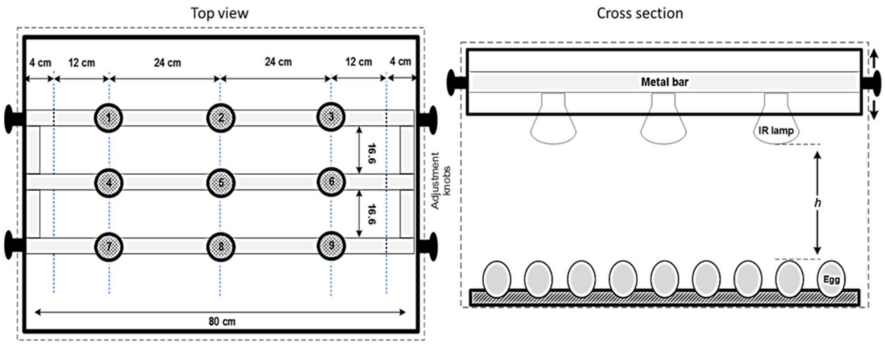

Figure 2. Schematic representation of the infrared cover showing the nine IR lamps (top view graph) and the adjustable distance from the eggs (h) using the adjustment knob (cross section graph).

2.2. Measurements and Data Acquisition

Measurements from incubator's built-in air temperature/humidity probe and CO_2 were recorded every two minutes and saved together with the controller set points in the data acquisition PC. The egg tray was spatially divided (through the short side) into three regions, each of which consisted of 50 eggs and facing one corresponding group of three IR lamps (Figure 3). In each region, two thermocouples (type-T) were placed on the equators of two eggs to represent the average eggshell temperature within each region (Figure 3). All the sensors were covered with aluminium foil for protection from overheating caused by the direct exposition to radiation heating.

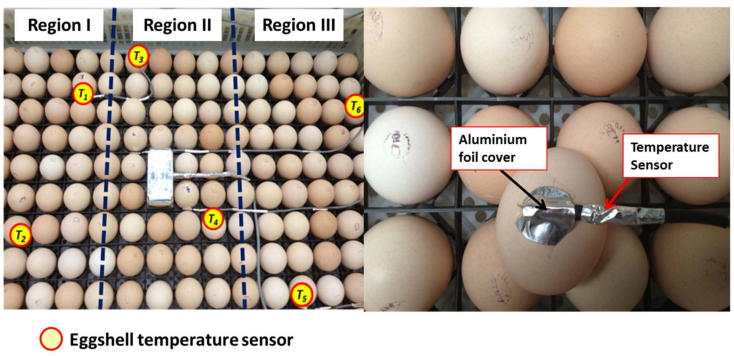

Figure 3. The location of the eggshell temperature sensors within each region (I, II and III) in the experimental incubator (left picture) and the temperature sensor placed on the equator of the eggshell covered with an aluminium foil to be protected from the IR heating (right picture).

2.3. Experiments

2.3.1. Pilot Experiments

In total, 12 pilot experiments were conducted to investigate the thermal profile (i.e., the main effective diameter of thermal radiation over the eggs surface, which is a function of the distance h between the lamp and the eggs) of the IR lamps. Additionally, these pilot experiments were conducted to investigate the maximal allowable operating power applied to the IR lamps to avoid over heating of the incubated eggs (to define the controller constraints). To investigate the thermal profile of the IR lamps over the incubated eggs a thermal camera (VarioCAM®, *InfraTech*) with 640 × 480 thermal resolution, is used. Two infertile eggs were placed on a small tray and one IR lamp was suspended from the top with an adjustable distance (h) from the surface of the two eggs.

Two infertile eggs ("equipped eggs") were equipped with two thermocouples. One thermocouple was fixed to the eggshell on the equator to measure the eggshell temperature (T_{egg}) and another was inserted 2 cm inside the egg, through a drilled hole in the narrow end of the egg (Figure 4), to measure the egg core temperature. The equipped eggs (Figure 4) were used to investigate how much the egg's internal temperature differs from the eggshell temperature and how fast the heat transferred from the eggshell to the internal parts of the eggs when using the IR heating. This enables the definition of the optimal constraints necessary for designing the IR controller to avoid any harms to the living embryo during incubation.

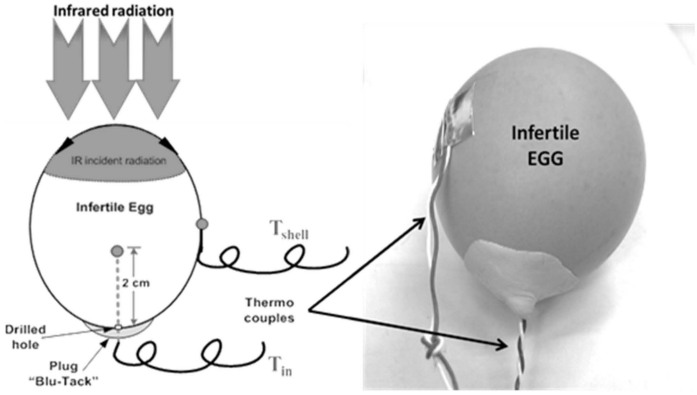

Figure 4. The "equipped egg" is an infertile egg, which was equipped with two thermocouples (type-T), one being placed on the equator of the egg, and the other one placed inside the egg through a drilled hole in the narrow end of the egg.

2.3.2. Control and System Identification Experiments

During the course of the research work reported in this paper, a set of five-step experiments were conducted to model the dynamic responses of eggshell temperatures to changes in the power (pulse width modulation, or PWM) applied to the IR radiators. The main goal was to develop a model predictive controller (MPC) to regulate, locally, the eggshell temperature of the incubated eggs within the incubator. The power applied to the IR radiators was manipulated by changing the duty cycle (percentage) of the PWM signals. The step experiments were carried out by applying step changes in the PWM duty cycle (percentage) to the IR radiators over the range 10–20%, while maintaining a fixed distance (h = 0.15 m, obtained from the pilot experiments) between the radiators and the eggs and constant air temperature (T_{air} ≈34 °C). Figure 5 shows an example of the applied step changes in the power applied to the IR radiators and the corresponding dynamic response of the eggshell temperature for two incubated eggs in region II.

2.3.3. Full Incubation Trials and Controller Implementation

Four full incubation trials were carried out to implement the developed MPCs. In order to test the performance of the developed predictive controllers in regulating the eggshell temperatures within the three regions (I, II and III) of the experimental incubator, 150 eggs were incubated with 50 eggs per region until hatching. During each incubation trial, reference trajectories of different set points were applied to evaluate the performance of each controller. To test the capability of the developed MPCs to create different thermal zones of eggshell temperature within the IRinc1 the reference trajectories to the three MPC's were defined in such a way that the eggshell temperatures within the middle regions (region II) was kept different (from day 10 until day 6) from the two sidelong regions (regions I and III).

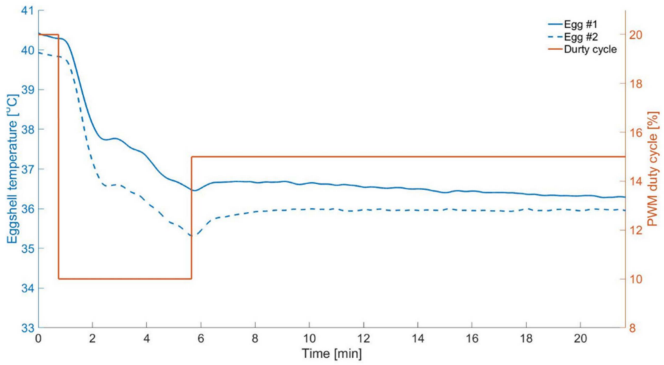

Figure 5. Step changes in the pulse width modulation (PWM) duty cycle (%) and the corresponding responses of the eggshell temperatures of two eggs in region II.

2.4. Model Predictive Controller (MPC) and System Identification

The proposed control strategy in this paper is based on controlling the temperature of the incubated eggs by combining the convective and radiative heating mechanisms (Figure 6). The forced convective heating/cooling was controlled using the Petersime Focus^{TM} controller and set to maintain the air temperature (T_{air}), within the main chamber, at a lower value (set point ≈ 34 °C) than the standard temperature for egg incubation (T_{std} = 37.8 °C). The radiative heating, using the IR radiators, was used to bring the eggshell temperature (T_{egg}) to the desired reference value $R_{Tegg}(k)$ at time k. A model predictive controller (MPC) was developed with the objective of maintaining the eggshell temperature (T_{egg}) around a certain predefined desired reference trajectory (R_{Tegg}) along the incubation period, which was achieved by actively manipulating the power applied to the IR radiators. The input power applied to the IR radiators was implemented through the pulse-widths modulated (PWM) signals generated using NI USB6251 interface.

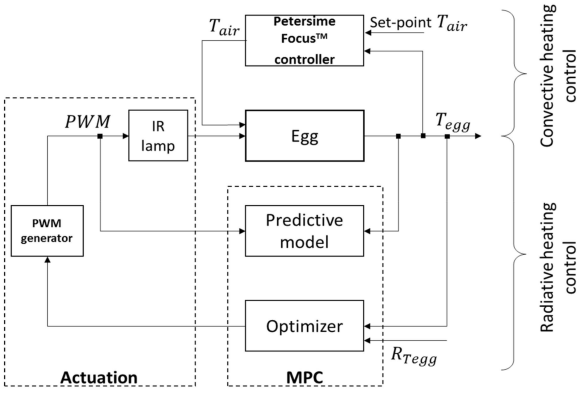

Figure 6. Block diagram representing the control strategy to combine both convective and radiative heating to control the eggshell temperature using model-predictive-controller (MPC) to regulate the eggshell temperature of incubated eggs.

2.4.1. System Identification and Parameter Estimation

A single-input, single-output (SISO) discrete transfer function (DTF) model was used to describe the static and dynamic responses of the eggshell temperature (T_{egg}) to step changes in the power (PWM duty cycle '%') applied to the IR radiators. The model has the following general structure [23]:

$$T_{egg}(k) = \frac{\boldsymbol{B}\left(\boldsymbol{z^{-1}}\right)}{\boldsymbol{A}\left(\boldsymbol{z^{-1}}\right)} u(k-\delta) - \xi(k) \tag{1}$$

where: $T_{egg}(k)$ is the output (average eggshell temperature per region) at time k; $u(k)$ is the input (PWM duty cycle to the IR radiators) at time k (min); $\xi(k)$ is additive noise, assumed to be a zero mean, serially uncorrelated sequence of random variables with variance σ^2 accounting for measurement noise, modelling errors and effects of unmeasured inputs to the process.

The two polynomials $\boldsymbol{A}\left(\boldsymbol{z^{-1}}\right)$ and $\boldsymbol{B}\left(\boldsymbol{z^{-1}}\right)$ are given by:

$$\begin{aligned} \boldsymbol{A}\left(\boldsymbol{z^{-1}}\right) &= 1 + a_1 z^{-1} + a_2 z^{-2} + \ldots + a_n z^{-na} \\ \boldsymbol{B}\left(\boldsymbol{z^{-1}}\right) &= b_0 + b_1 z^{-1} + b_2 z^{-2} + \ldots + b_m z^{-nb} \end{aligned} \tag{2}$$

where a_i and b_i are the model parameters to be estimated; z^{-i} is the backward shift operator, $z^{-1} \cdot y(k) = y(k-1)$; and n, m are the orders of the respective polynomials. In the present paper, the simplified refined Instrumental variable (SRIV) algorithm was utilised in the identification and estimation of the models [24]. The appropriate model structure was identified, i.e., the most appropriate values for the triad [n, m, δ] (see Equation (1)). Two main statistical measures were employed to determine the most appropriate values of this triad. Namely, the coefficient of determination R_2^T, based on the response error; and *YIC* (Young's information criterion), which provides a combined measure of model fit and parametric efficiency, with large negative values indicating a model which explains the output data well and yet avoids over-parameterisation [25,26].

2.4.2. MPC and Cost Function Formulation

The general idea behind any MPC design is to select a sequence of N_c future control moves to minimise a cost function J (Equation (3)) over a prediction horizon of N_p sample times [27]. In this paper, a quadratic programming cost function with quadratic objective function and linear constraints was used. The quadratic programming form leads to smoother control actions in comparison to the linear form. The model predictive controller uses the model (Equation (1)) to predict the response of the system based on the past measured inputs and outputs. This predicted output ($\hat{T}_{egg}$) was then used to calculate the optimal input by mathematical optimisation techniques in order to reduce the difference between this output and the desired one (R_{Tegg}). This optimal input was calculated by minimizing the following cost function [21]:

$$J\left(N_1, N_p, N_c\right) = \sum_{j=N_1}^{N_p} \alpha_j \left[\hat{T}_{egg}\left(k+j\middle|k\right) - R_{Tegg}[k+j]\right]^2 + \sum_{j=1}^{N_c} \lambda_j [\Delta u[k+j-1]]^2 \tag{3}$$

where, $\Delta u(k)$ is the change in input (power applied to the IR radiators), $\hat{T}_{egg}(k+j|k)$ is the predicted output (eggshell temperature) sequence, $R_{Tegg}(k)$ is the desired value of the output, N_1 is the minimum of the prediction horizon, α and λ are the weighting factors. The block diagram depicted in Figure 7. shows the basic structure of the designed MPC system in the present work to control the eggshell temperature using localised IR heating.

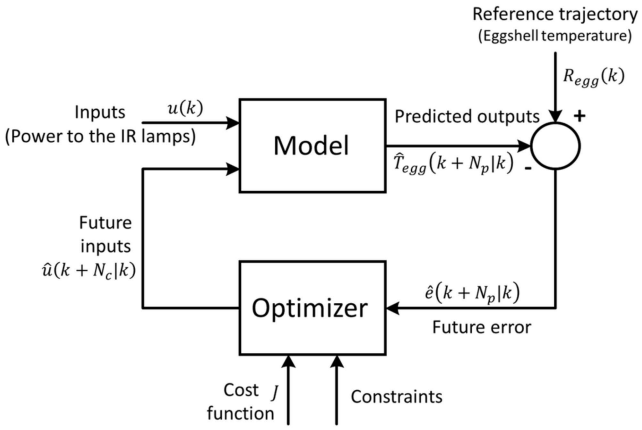

Figure 7. Block diagram representing the basic structure of the proposed MPC system to control the eggshell temperature of incubated eggs.

The model (Equation (1)) is the cornerstone of the MPC system and should be robust enough to fully capture the process dynamics [21]. In other words, the identified model should be able to describe the dynamic responses of the eggshell temperature to changes in the control input (i.e., power applied to the IR radiators). There is a wide family of MPC algorithms, each member of which is defined by the choice of the prediction model, the cost function and obtaining the control law [21]. In the present paper, the dynamic matrix control (DMC) algorithm was considered. The DMC formulation uses the step response to model the process [21,28]. The process model employed in this formulation is the step response of the eggshell temperature to step increase in the input, while the disturbance was considered constant along the prediction horizon (N_p). The procedure to obtain the predictions is as follows. As a *step response* model (Equation (1)) was employed:

$$T_{egg}(k+j) = \sum_{j=1}^{\infty} g_j \Delta u(k+j-1) \tag{4}$$

where g_j is the *step response* coefficient.

The predicted eggshell temperature along the prediction horizon is:

$$\hat{T}_{egg}(k+j|k) = \sum_{j=1}^{N_p} g_j \Delta u(k+j-1) + f(k+j) \tag{5}$$

where the $f(k+j)$ is the *free response* of the system.

Equation (5) can be written as follows:

$$\begin{bmatrix} \hat{T}_{egg}[k+1|k] \\ \hat{T}_{egg}[k+2|k] \\ \cdots \\ \hat{T}_{egg}\left[k+N_p|k\right] \end{bmatrix} = \begin{bmatrix} g_1 & 0 & \cdots & 0 \\ g_2 & g_1 & \cdots & 0 \\ \vdots & \vdots & \ddots & \vdots \\ g_{N_p} & g_{N_p-1} & \cdots & g_1 \end{bmatrix} \cdot \begin{bmatrix} \Delta u[k] \\ \Delta u[k+1] \\ \cdots \\ \Delta u[k+N_c-1] \end{bmatrix} + \begin{bmatrix} f[k] \\ f[k+1] \\ \cdots \\ f\left[k+N_p-1\right] \end{bmatrix} \tag{6}$$

or

$$\hat{\boldsymbol{T}} = \mathbf{G}\mathbf{u} + \mathbf{f} \tag{7}$$

where $\mathbf{G}$ is the $N_p \times N_c$ *dynamic matrix*, $\hat{\boldsymbol{T}}$ is the N_p-dimension vector contains the predicted eggshell temperatures along the prediction horizon, $\mathbf{u}$ represents the N_c-dimension vector of the control inputs and $\mathbf{f}$ is the *free response* vector. Hence, using Equation (7) the cost Function (3) can be represented in the following form [21]:

$$J = (\mathbf{G}\mathbf{u} + \mathbf{f} - \mathbf{R})^{\mathrm{T}}(\mathbf{G}\mathbf{u} + \mathbf{f} - \mathbf{R}) + \lambda \mathbf{u}^{\mathrm{T}}\mathbf{u} \tag{8}$$

$$J = \frac{1}{2}\mathbf{u}^{\mathrm{T}}\mathbf{H}\mathbf{u} + \mathbf{b}^{\mathbf{T}}\mathbf{u} + \mathbf{f}_0 \tag{9}$$

with $\mathbf{H} = 2\left(\mathbf{G}^T\mathbf{G} + \lambda\mathbf{I}\right)$, $\mathbf{b}^T = 2(\mathbf{f} - \mathbf{R})^T\mathbf{G}$ and $\mathbf{f}_0 = (\mathbf{f} - \mathbf{R})^T(\mathbf{f} - \mathbf{R})$.

The cost Function (9) is quadratic, therefore, the minimum is unique. The optimal input change can be calculated by setting the derivative equal to zero:

$$\frac{dJ}{d\mathbf{u}} = 2\left(\mathbf{G}^{\mathrm{T}}\mathbf{G} + \lambda\mathbf{I}\right)\mathbf{u} + 2\mathbf{G}^{\mathrm{T}}(\mathbf{f} - \mathbf{R}) = 0 \tag{10}$$

Then the optimal input change is given by:

$$\mathbf{u} = \left(\mathbf{G}^{\mathrm{T}}\mathbf{G} + \lambda\mathbf{I}\right)^{-1}\mathbf{G}^{\mathrm{T}}(\mathbf{R} - \mathbf{f}) \tag{11}$$

For the control law, as such, only the first element of vector **u** was implemented.

3. Results

3.1. Pilot Experiments

The results of the conducted experiments have shown that the optimal thermal profile of the IR lamps was achieved at distance (h) of 0.15 m, which corresponds to an effective diameter of 0.30 m.

Figure 8 shows a comparison between the temperature responses of the equipped eggs under convective heating and radiative heating (at PWM of 10%). The results (an example is shown in Figure 8) have shown that the temperature difference between the egg-core and the eggshell was vanishing (quasi zero) faster (5.2 ± 1.5 min) in case of radiative heating in comparison to convective heating (9.4 ± 1.8 min). The average time constants of eggshell temperature in case of radiative and convective heating were 7.6 ± 1.2 min and 7.45 ± 1.23 min, respectively. The steady-state eggshell temperature at different power levels (PWM) applied to the radiative lamps are shown in Figure 9. A linear regression model was fit the relation between the eggshell temperature (°C) and PWM (%) with a slope of 0.42.

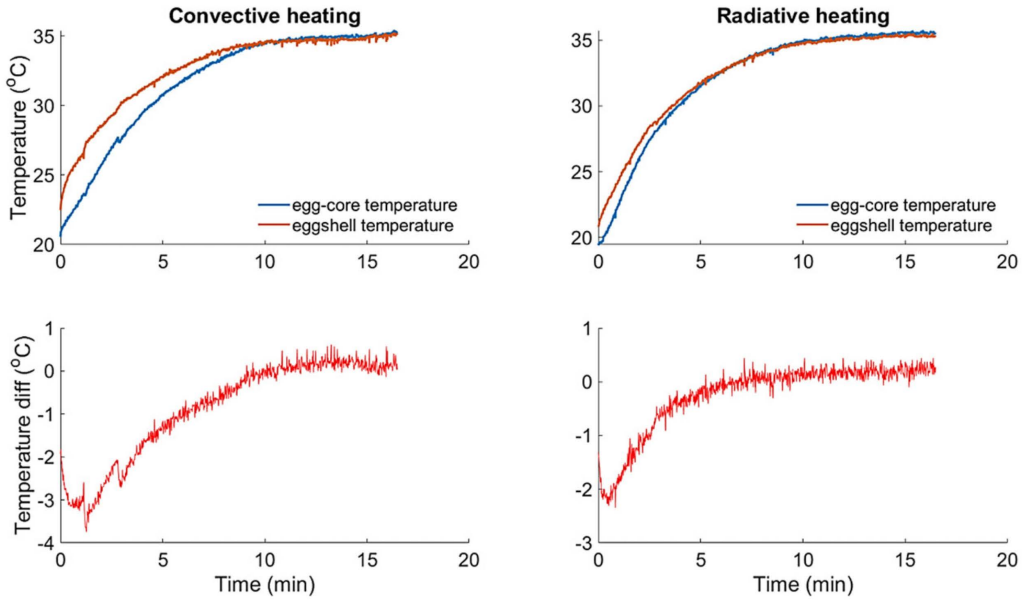

Figure 8. Step responses of eggshell and egg core temperatures to step up increases in convective-heating (left graphs) and radiative-heating (right graphs), with PWM = 10%, inside the experimental incubator. The 'temperature diff' is the difference between the egg-core and the eggshell temperatures.

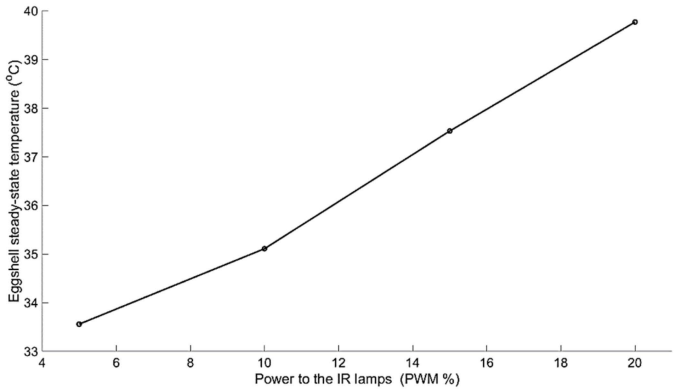

Figure 9. The resulted steady-state temperature of the eggshell at different PWM (%) to the IR lamps at distance h = 0.15 m.

3.2. System Identification and Predictive Model Generation

It should be stated here that the objective of this stage was to identify an approximation mode of the incubated fertile-egg system. The identification step in the present paper was tuned towards the main objective of control-oriented model design.

The SRIV algorithm, combined with the *YIC* and R_2^T, suggested that a second-order (number of poles, n = 2) DTF model with one minute pure delay (δ = 1 min) was most suitable (i.e., R_2^T = 0.98 ± 0.01 and *YIC* = −13.00 ± 1.45) to describe the dynamic responses of the eggshell temperature ($T_{egg}(k)$) to step changes in the power applied to the IR radiators ($u(k)$). More specifically, the SRIV algorithm identified the following general DTF model structure (denoted by the triad [2 2 2], i.e., n = 2, m = 2 and δ = 2),

$$T_{egg}(k) = \frac{b_1 z^{-1} + b_2 z^{-2}}{1 + a_1 z^{-1} + a_2 z^{-2}} u(k-\delta) \tag{12}$$

or in the following difference equation form,

$$T_{egg}(k) = -a_1.T_{egg}(k-1) - a_2.T_{egg}(k-2) + b_1.u(k-\delta-1) + b_2.u(k-\delta-2) \tag{13}$$

Table 1 shows the average parameter estimates for the identified model structure for the three eggs.

Table 1. The resulted model parameter estimates (average and ± standard error) obtained from 15 incubated eggs at embryonic day (ED) 15.

$A(z^{-1})$		$B(z^{-1})$		R_T^2	*YIC*
a_1	a_2	b_1	b_2	0.98 (± 0.01)	−13.00 (± 1.45)
−1.997 (± 0.003)	0.997 (± 0.003)	0.0010 (± 0.0017)	−0.0010 (± 0.0017)		

3.3. Model Predictive Control Design

3.3.1. MPC Cost Function and Constraints

During the incubation process, the thermoregulatory system of the chicken embryo evolves through different stages from a poikilothermic to a homeothermic system. Hence, the thermal response of the fertile egg to changes in ambient temperature is different from one day to another during the embryonic development [15]. Such a complex and sensitive process is subject to a number of limitations and constraints pertaining to the ranges of tolerable eggshell temperatures and acceptable IR operating power range. Table 2 shows the applied constraints on the controlled, T_{egg}, and the manipulated, $u(k)$, variables during designing the MPC system. Based on the results of pilot experiments, the control signal, $u(k)$, was constrained within the allowable PWM range between 0 and 20%. In order to prevent large increments in the rate of change in the manipulated variable $\Delta u(k)$, the maximum boundary was

set as small as 0.5%. On the other hand, to prevent overheating a fast decrease in the IR heating was allowed by setting the minimum boundary to −2%. Additionally, the controlled variable, $T_{egg}(k)$, was constrained within the allowable incubation range between 36 and 40 °C.

Table 2. The predefined constraints on both the controlled and manipulated variables, which should be considered for designing the MPC system.

	Constraints
Manipulated variable (power to the IR, PWM, %)	$u(k) = (0, 20)$
Change in the Manipulated variable (%)	$\Delta u(k) = (-2, 0.5)$
Controlled variable (average eggshell temperature, °C)	$T_{egg}(k) = (34, 40)$

The developed MPC system should anticipate constraint violations and correct them in an appropriate way. Therefore, the minimization of the cost Function (9) is subject to constraints on the output ($T_{egg}(k)$, eggshell temperature), input ($u(k)$, power applied to the IR radiators) and changes in the input, $\Delta u(k)$, as the quadratic programing (QP) formulation:

$$\min_{\mathbf{u}} \frac{1}{2}\mathbf{u}^{\mathrm{T}}\mathbf{H}\mathbf{u} + \mathbf{b}^{\mathrm{T}}\mathbf{u}, \text{subject to} \begin{cases} 0 \leq u\{k \leq 20 \\ -2 \leq \Delta u\{k \leq 0.5 \\ 34 \leq T_{egg}\{k \leq 40 \end{cases} \quad (14)$$

3.3.2. MPC Simulation

To simulate the closed-loop MPC of the eggshell temperature (controlled variable, $T_{egg}(k)$) using the power applied to the IR radiators (manipulated variable, $u(k)$) the following design parameters were defined:

1. Sampling time (or period) t_s, which determines the rate at which the control algorithm was executed. The shorter the sampling period the better controller performance to deal with fast disturbances. On the other hand, diminishing t_s can increase the computational burden. In any case, t_s should not exceed the maximal expected time necessary for running one iteration of the MPC algorithm [29]. In the current study the sampling time was chosen to be one sample (t_s = 1 min), which corresponds to a value ten times smaller than the average observed rise time (t_r = 10.12 ± 0.22 min).
2. Defining the prediction and control horizons, which should be at least same or larger than the settling time of the system. The control horizon in general should be less than the defined prediction horizon and based on many applications an optimal control horizon should be between 20–30% of the prediction horizon to ensure smooth control actions and yet low computational costs. In the current study, the prediction N_p and control N_c horizons were set to 20 samples (N_p > average settling time = 16.20 ± 1.13 min) and five samples (25% of the prediction horizon).
3. To achieve a balanced performance between the competing control objectives (i.e., a close tracking of the set-point together with smooth control moves), the weighting factors α and λ were set to 0.9 and 0.8, respectively [30], to avoid any conflict between the control objectives.

The controller algorithm is initialized by computing the *dynamic matrix* **G** for the system (13), which is defined, based on (6), as follows:

$$\mathbf{G} = \begin{bmatrix} g_1 & 0 & 0 \\ g_2 & g_1 & 0 \\ g_3 & g_2 & g_1 \end{bmatrix} \quad (15)$$

where,

$$g_1 = -a_1.T_{egg}(k-1) - a_2.T_{egg}(k-2) + b_1.u(k-\delta-1) + b_2.u(k-\delta-2)$$
$$g_2 = -a_1.T_{egg}(k) - a_2.T_{egg}(k-1) + b_1.u(k-\delta) + b_2.u(k-\delta-1)$$
$$g_3 = -a_1.T_{egg}(k+1) - a_2.T_{egg}(k) + b_1.u(k-\delta+1) + b_2.u(k-\delta)$$

and computing the control *gain matrix* **K**, which is defined as follows:

$$\mathbf{K} = \left(\mathbf{G}^{\mathrm{T}}\mathbf{G} + \lambda\mathbf{I}\right)^{-1}\mathbf{G}^{\mathrm{T}}$$

A zero mean ($\mu = 0$) white noise term with variance (σ) of 0.1 was added to both output $T_{egg}(k)$ and input $u(k)$ signals to simulate the measurement and actuator noises (unmeasured disturbances), respectively. A simulation example of the closed-loop response of the designed MPC controller based on the DTF model (12) is depicted in Figure 10. Despite the added disturbances in both input and output signals, the simulation of the MPC closed-loop response was able to follow the reference signal (set point) efficiently with max error ($T_{egg} - R_{Tegg}$) of ±0.4 °C.

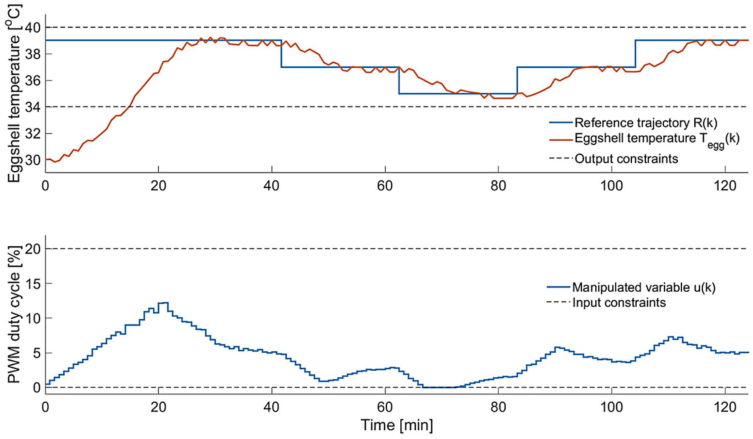

Figure 10. A simulation example of the closed-loop step response $T_{egg}(k)$ (upper graph) and unmeasured disturbances in both input and output using the designed constrained MPC controller based on the general TF model structure (12), showing the control signal $u(k)$ (lower graph). The closed-loop simulation of the developed MPC was implemented on MATLAB on a computer with Intel® 8 core i7 (2.7 GHz) processor and 16GB RAM. The average computational time for one iteration on this computer was 15.6 s.

3.3.3. MPC Implementation and Full Incubation Experiments

A two-level zonal control system was developed combining both convective and radiative heating to regulate the eggshell temperatures within three different zones (region I, II and III) simultaneously. On the higher-level three MPC systems were used to regulate the eggshell temperatures within the three regions. Additionally, a PID controller (Petersime Focus™) was employed in the lower level to regulate the incubation air temperature within the experimental incubator.

Four full incubation trials were carried out to implement and tune the developed MPC system to regulate the eggshell temperatures of incubated eggs in three different zones inside the experimental incubator (see Figure 11). To investigate the possibility of the controllers to regulate the eggshell temperatures within the three regions, the reference trajectory for region II (middle region) was different from those for sidelong regions (i.e., region I and III). The programmed reference trajectories were including some extreme set points (e.g., 34 °C), which do not follow the standard eggshell temperature (around 38 °C). Therefore, it was expected that such treatments might affect the final hatching results. Figure 11 shows an example of the implementation results of the developed MPCs to regulate the eggshell temperatures inside the experimental incubator IRin1. By employing different set points,

it was possible to create two thermal zones, between days 0 and 6, (at region I and III) of incubated eggs with more or less same eggshell temperature sandwiching another with different eggshell temperature.

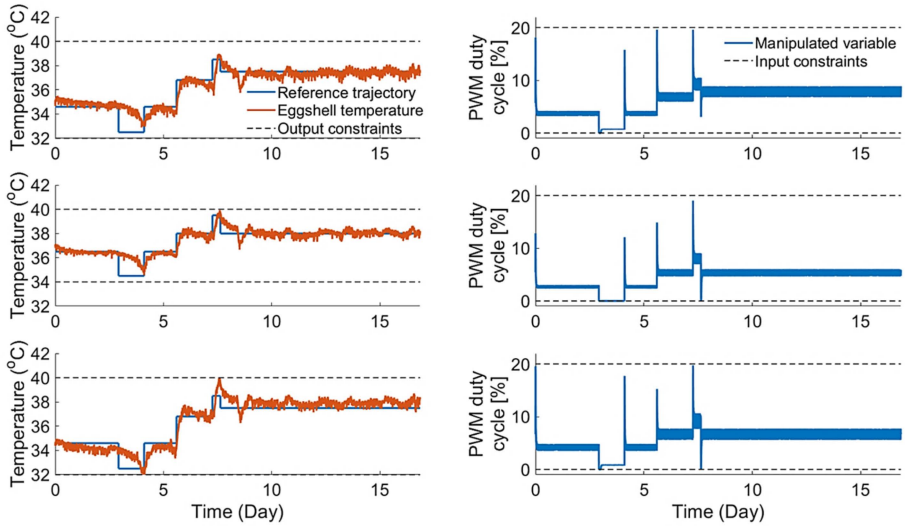

Figure 11. Example of the implementation results of the developed MPCs to regulate the eggshell temperatures at three different regions, I (upper graphs), II (middle graphs) and II (lower graphs) simultaneously.

Although the controllers were able to follow the reference trajectories in each zone (region), it was noticed (Figure 11) that the responses of the eggshell temperatures in each zone exhibited an oscillation around the set point values with an average error of ±0.5 °C. This can be attributed to the unmeasured disturbances resulting from the interaction between adjacent zones with different temperatures and to the control actions of the PID (Petersime Focus^{TM}) controller, which regulates the incubation air temperature around the eggs in the whole incubator. Another possible reason for such oscillated deviation between the actual eggshell temperature and the set point is the fact that, during this study, we have designed the MPCs based on one predictive model (12). That with the assumption that the DTF model (12) is representative of the controlled dynamic system (incubated embryo). However, in reality as shown in previous studies (e.g., [15]) the incubated embryo is inherently a nonlinear system, which exhibits different dynamics and responses almost every embryonic day. Therefore, we are proposing for future work an adaptive control approach, in which a linear model (with a fixed model structure as (12)) is estimated on the fly as the operation conditions are changing, hence the internal system-model of the MPC is updated at each scheduled time period (e.g., each day).

Previous studies (e.g., [31–34]) showed that the incubated chicken embryos are evolving at early stage of development (between incubation days ED 5–7) from an ectothermic (gaining its required heat from the surrounding environment) organism to an endothermic (produces its own heat) organism. Hence, in practice of industrial incubation, most of the energy is used to cool down the incubated embryo to the standard eggshell temperature (~38 °C). Therefore, the proposed two-level control system, which combine convective and radiative heating, is believed to be a promising technique to use the energy more efficiently during incubation. This can be achieved by locally heating up the required zones using localized IR heating (i.e., demand-based climate controlling). Additionally, a multi-objective cost function can be used to optimize the energy used by including an extra constraint on total energy consumption.

The results of the four full incubation trials showed that combining both convective and radiative heating mechanisms was successful to hatch the incubated eggs with average hatch-of-fertile (HOF = (hatched chicks/number of true fertile eggs) × 100) of 84.0% (±0.5). A breakout of the unhatched eggs was performed [35,36] in the end of each incubation trial. The average breakout results of the unhatched eggs are shown in Figure 12.

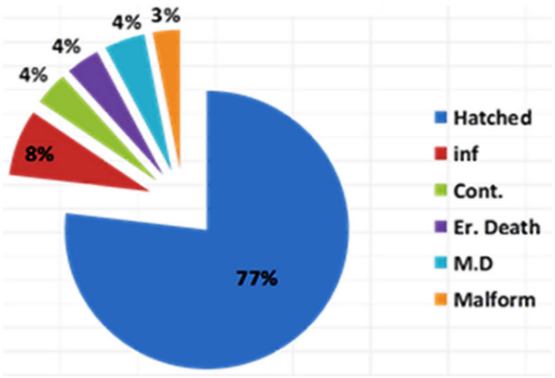

Figure 12. Average breakout results of the unhatched eggs during the four full incubation trials showing the percentage of hatched, infertile (inf), contaminated (Cont.), early death (Er. Death), middle death (M.D) and malformed embryo.

4. Conclusions

During the present study, a two-levels controller was designed and implemented to combine both convective and radiative heating to incubate eggs. On the higher level, three MPC constrained controllers were developed to regulate the power applied to nine IR-radiators divided into three zones based on continuous feedback of the eggshell temperatures in each zone. On the lower level, a PID controller (Petersime Focus^{TM}) was used to maintain the air temperature within an experimental incubator at a fixed level (34 °C) lower than the standard incubation temperature. Four full incubation trials were carried out to test and implement the developed zonal controllers. The implementation results showed that the developed controllers were able to follow the reference trajectory defined for each zone. It was possible to keep the eggshell temperatures within the middle region (zone) different from the sidelong regions (zones) while the air temperature kept fixed at 34 °C. The average hatching result (HOF) of the four full incubation trial was 84.0% (±0.5). The developed two-levels control system is a promising technique for demand-based climate controller and to optimize energy use by using multi-objectives MPCs with constraint on total energy consumption.

Author Contributions: Conceptualization, A.Y. and D.B.; methodology, A.Y.; software, A.Y.; validation, A.Y.; formal analysis, A.Y.; investigation, A.Y.; resources, D.B. and T.N.; data curation, A.Y.; writing—original draft preparation, A.Y.; writing—review and editing, A.Y. and T.N.; visualization, A.Y.; supervision, A.Y., T.N. and D.B.; project administration, T.N. and D.B.; funding acquisition, D.B.

Funding: This research was funded by the Belgian government agency for Innovation by Science and Technology (IWT), grant number IWT110404: 2011–2014.

Acknowledgments: The authors gratefully thank to the technical and financial support of Petrsime N.V. (Belgium) and the support of Petersime R&D team, namely, Luc Gabrial, Rudy Verhelst, Pascal Garain and Paul Degraeve.

Conflicts of Interest: The authors declare no conflict of interest.

References

1. OECD/FAO. *OECD-FAO Agricultural Outlook 2019–2028*; OECD: Paris, France, 2017.
2. Fasenko, G.M. Egg Storage and the Embryo. *Poult. Sci.* **2013**, *86*, 1020–1024. [CrossRef] [PubMed]
3. Bergoug, H.; Burel, C.; Guinebretiere, M.; Tong, Q.; Roulston, N.; Romanini, C.E.; Exadaktylos, V.; McGonnell, I.M.; Demmers, T.G.; Verhelst, R.; et al. Effect of pre-incubation and incubation conditions on hatchability, hatch time and hatch window, and effect of post-hatch handling on chick quality at placement. *World's. Poult. Sci. J.* **2013**, *69*, 313–334. [CrossRef]
4. Uni, Z.; Noy, Y.; Sklan, D. Posthatch development of small intestinal function in the poult. *Poult. Sci.* **1999**, *78*, 215–222. [CrossRef] [PubMed]
5. Noy, Y.; Sklan, D. Yolk and Exogenous Feed Utilization in the Posthatch Chick. *Poult. Sci.* **2001**, *80*, 1490–1495. [CrossRef] [PubMed]

6. Romanini, C.E.; Exadaktylos, V.; Tong, Q.; McGonnel, I.; Demmers, T.G.; Bergoug, H.; Eterradossi, N.; Roulston, N.; Garain, P.; Bahr, C.; et al. Monitoring the hatch time of individual chicken embryos. *Poult. Sci.* **2013**, *92*, 303–309. [CrossRef] [PubMed]
7. Tong, Q.; McGonnell, I.M.; Roulston, N.; Bergoug, H.; Romanini, C.E.; Garain, P.; Eterradossi, N.; Exadaktylos, V.; Bahr, C.; Berckmans, D.; et al. Higher levels of CO_2 during late incubation alter the hatch time of chicken embryos. *Br. Poult. Sci.* **2015**, *56*, 503–509. [CrossRef] [PubMed]
8. Gucbilmez, M.; Ozlu, S.; Shiranjang, R.; Elibol, O.; Brake, J. Effects of preincubation heating of broiler hatching eggs during storage, flock age, and length of storage period on hatchability. *Poult. Sci.* **2013**, *92*, 3310–3313. [CrossRef]
9. Hulet, R.; Gladys, G.; Hill, D.; Meijerhof, R.; El-Shiekh, T. Influence of egg shell embryonic incubation temperature and broiler breeder flock age on posthatch growth performance and carcass characteristics. *Poult. Sci.* **2007**, *86*, 408–412. [CrossRef]
10. Lourens, A. *Embryo Temperature during Incubation: Practice and Theory*; Wageningen University: Wageningen, The Netherlands, 2008.
11. Shelehov, I.Y.; Smirnov, E.I.; Inozemsev, V.P. Localized Electrical Heating System for Various Types of Buildings. *IOP Conf. Ser. Mater. Sci. Eng.* **2017**, *262*, 012083. [CrossRef]
12. Youssef, A.; Exadaktylos, V.; Ozcan, S.E.; Berckmans, D. Proportional-Integral-Plus (PIP) Control System for Individual Thermal Zones in a Small Ventilated Space. *ASHRAE Trans.* **2011**, *117*, 48–56.
13. Youssef, A.; Yen, H.; Özcan, S.E.; Berckmans, D. Data-based mechanistic modelling of indoor temperature distributions based on energy input. *Energy Build.* **2011**, *43*, 2965–2972. [CrossRef]
14. Janssens, K.; van Brecht, A.; Desta, T.Z.; Boonen, C.; Berckmans, D. Modeling the internal dynamics of energy and mass transfer in an imperfectly mixed ventilated airspace. *Indoor Air* **2004**, *14*, 146–153. [CrossRef] [PubMed]
15. Youssef, A.; Exadaktylos, V.; Berckmans, D. Modelling and quantification of the thermoregulatory responses of the developing avian embryo: Electrical analogies of a physiological system. *J. Therm. Biol.* **2014**, *44*, 14–19. [CrossRef] [PubMed]
16. Tzschentke, B.; Rumpf, M. Embryonic development of endothermy. *Respir. Physiol. Neurobiol.* **2011**, *178*, 97–107. [CrossRef] [PubMed]
17. Quanten, S.; de Valck, E.; Cluydts, R.; Aerts, J.-M.; Berckmans, D. Individualized and time-variant model for the functional link between thermoregulation and sleep onset. *J. Sleep Res.* **2006**, *15*, 183–198. [CrossRef] [PubMed]
18. Youssef, A. *Model-Based Control of Micro-Environment with Real-Time Feedback of Bioresponses*; KU Leuven: Leuven, Belgium, 2014.
19. Trentelman, H.L.; Stoorvogel, A.A.; Hautus, M. *Control Theory for Linear Systems*; Springer: London, UK, 2001.
20. Leigh, J.R. *Applied Control Theory*; Rev Sub. P. Peregrinus Ltd. on behalf of the Institution of Electrical Engineers: London, UK, 1987.
21. Camacho, E.F.; Bordons, C. *Model Predictive Control*; Springer: London, UK, 2007.
22. Kaiser, E.; Kutz, J.N.; Brunton, S.L. Sparse identification of nonlinear dynamics for model predictive control in the low-data limit. *Proc. R. Soc. A Math. Phys. Eng. Sci.* **2018**, *474*, 20180335. [CrossRef] [PubMed]
23. Godina, R.; Rodrigues, E.M.G.; Pouresmaeil, E.; Catalão, J.P.S. Optimal residential model predictive control energy management performance with PV microgeneration. *Comput. Oper. Res.* **2018**, *96*, 143–156. [CrossRef]
24. Young, P.C.; Chotai, A.; Tych, W. *Identification, Estimation and Control of Continuous-Time Systems Described by Delta Operator Models*; Kluwer Academic Publishers: Dordrecht, The Netherlands, 1991.
25. Young, P.C.; Jakeman, A. Refined instrumental variable methods of recursive time-series analysis Part III. Extensions. *Int. J. Control* **1980**, *31*, 741–764. [CrossRef]
26. Young, P.C. *Recursive Estimation and Time-Series Analysis: An Introduction for the Student and Practitioner*; Springer: Berlin/Heidelberg, Germany, 2011.
27. Camacho, E.F.; Bordons, C. Model Predictive Control. *Int. J. Robust Nonlinear Control* **1999**, *13*, 280.
28. Cutler, C.R.; Ramaker, B.C. Dynamic Matrix Control? A Computer Control Algorithm. *Autom. Control Conf.* **1980**, *17*, 72. [CrossRef]
29. Wysocki, A.; Ławryńczuk, M. On Choice of the Sampling Period and the Horizons in Generalized Predictive Control. In *Recent Advances in Automation, Robotics and Measuring Techniques*; Springer: Cham, Switzerland, 2014; pp. 329–339.

30. Borrelli, F.; Bemporad, A.; Morari, M. *Predictive Control for Linear and Hybrid Systems*; Cambridge University Press: New York, NY, USA, 2017.
31. Mueller, C.A.; Burggren, W.W.; Tazawa, H. The Physiology of the Avian Embryo Chapter 32. In *Sturkie's Avian Physiology*; Academic Press: Cambridge, MA, USA, 2015; pp. 739–766.
32. Whittow, G.C.; Tazawa, H. The early development of thermoregulation in birds. *Physiol. Zool.* **2002**, *64*, 1371–1390. [CrossRef]
33. Janke, O.; Tzschentke, B.; Höchel, J.; Nichelmann, M. Metabolic responses of chicken and muscovy duck embryos to high incubation temperatures. *Comp. Biochem. Physiol. Part A Mol. Integr. Physiol.* **2002**, *131*, 741–750. [CrossRef]
34. Tzschentke, B. Monitoring the development of thermoregulation in poultry embryos and its influence by incubation temperature. *Comput. Electron. Agric.* **2008**, *64*, 61–71. [CrossRef]
35. Fayeye, T.; Olapade, A. Hatch-Out Analysis and Repeatability Estimates of Common Hatchability Problems in Issa-Brown Breeder Stock. *Agrosearch* **2013**, *13*, 51. [CrossRef]
36. Mauldin, J.M. Breakout Analyses Guide for Hatcheries|The Poultry Site. 2003. Available online: https://thepoultrysite.com/articles/breakout-analyses-guide-for-hatcheries-1 (accessed on 25 August 2019).